Fate of pristine TiO2 nanoparticles and aged paint-containing TiO2 nanoparticles in lettuce crop after foliar exposure

Camille Larue, Hiram Castillo-Michel, Sophie Sobanska, Nicolas Trcera, Stéphanie Sorieul, Lauric Cécillon, Laurent Ouerdane, Samuel Legros, Géraldine Sarret

Journal of Hazardous Materials 273 (2014) 17–26

Contents lists available at ScienceDirect

Journal of Hazardous Materials

journal homepage: www.elsevier.com/locate/jhazmat

Fate of pristine TiO_2 nanoparticles and aged paint-containing TiO_2 nanoparticles in lettuce crop after foliar exposure

Camille Larue[a,*], Hiram Castillo-Michel[b], Sophie Sobanska[c], Nicolas Trcera[d], Stéphanie Sorieul[e], Lauric Cécillon[a], Laurent Ouerdane[f], Samuel Legros[g], Géraldine Sarret[a]

[a] ISTerre, Université de Grenoble 1, CNRS, 38041 Grenoble, France
[b] European Synchrotron Radiation Facility, Beamline ID21, Grenoble, France
[c] Laboratoire de Spectrochimie Infra Rouge et Raman, UMR CNRS 8516, Université Lille 1, Bât C5, 59655 Villeneuve d'Ascq Cedex, France
[d] Synchrotron SOLEIL, Gif-sur-Yvette 91192, France
[e] Université Bordeaux 1, CNRS/IN2P3, Centre d'Etudes Nucléaires de Bordeaux Gradignan, CENBG, Chemin du Solarium, BP120, 33175 Gradignan, France
[f] Laboratoire de Chimie Analytique Bio-Inorganique et Environnement, Institut Pluridisciplinaire de Recherche sur l'Environnement et les Matériaux (LCABIE/IPREM-UMR 5254), Université de Pau et des Pays de l'Adour, Hélioparc, 2 Av. Pierre Angot, 64053 Pau Cedex 9, France
[g] CEA/LITEN/DTNM/L2T, CEA Grenoble, Av des Martyrs, 38054 Grenoble Cedex 9, France

HIGHLIGHTS

- Pristine TiO_2-NPs are internalized inside lettuce leaves after foliar exposure.
- TiO_2-NPs and microparticles from aged paint leachate are detected in plants after foliar exposure.
- The chemical form of TiO_2 particles is unchanged upon internalization.
- Foliar exposure to pristine TiO_2-NPs does not lead to acute phytotoxicity symptoms.

GRAPHICAL ABSTRACT

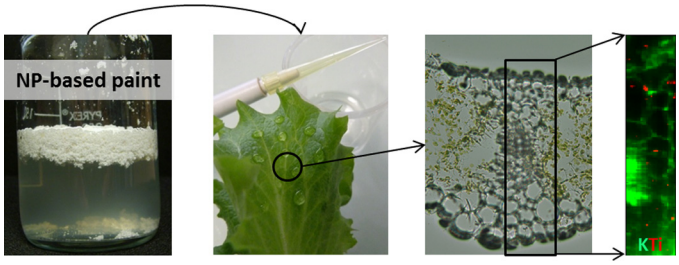

ARTICLE INFO

Article history:
Received 25 December 2013
Received in revised form 14 February 2014
Accepted 7 March 2014
Available online 24 March 2014

Keywords:
Ecotoxicology
Plant
TiO_2 nanoparticle
Micro-XRF
Micro-XAS

ABSTRACT

Engineered TiO_2 nanoparticles (TiO_2-NPs) are present in a large variety of consumer products, and are produced in largest amount. The building industry is a major sector using TiO_2-NPs, especially in paints. The fate of NPs after their release in the environment is still largely unknown, and their possible transfer in plants and subsequent impacts have not been studied in detail. The foliar transfer pathway is even less understood than the root pathway. In this study, lettuces were exposed to pristine TiO_2-NPs and aged paint leachate containing TiO_2-NPs and microparticles (TiO_2-MPs). Internalization and *in situ* speciation of Ti were investigated by a combination of microscopic and spectroscopic techniques. Not only TiO_2-NPs pristine and from aged paints, but also TiO_2-MPs were internalized in lettuce leaves, and observed in all types of tissues. No change in speciation was noticed, but an organic coating of TiO_2-NPs is likely. Phytotoxicity markers were tested for plants exposed to pristine TiO_2-NPs. No acute phytotoxicity was observed; variations were only observed in glutathione and phytochelatin levels but remained low as compared to typical values. These results obtained on the foliar uptake mechanisms of nano- and microparticles are important in the perspective of risk assessment of atmospheric contaminations.

* Corresponding author at: Lehrstuhl für Pflanzenphysiologie, Ruhr-Universität Bochum, Universitätsstraße 150, 44801 Bochum, Germany. Tel.: +49 234 32 24302.
E-mail addresses: camille.larue@rub.de, Camille.Larue@ruhr-uni-bochum.de (C. Larue), castillo@esrf.fr (H. Castillo-Michel), sophie.sobanska@univ-lille1.fr (S. Sobanska), nicolas.trcera@synchrotron-soleil.fr (N. Trcera), sorieul@cenbg.in2p3.fr (S. Sorieul), lauric.cecillon@irstea.fr (L. Cécillon), laurent.ouerdane@univ-pau.fr (L. Ouerdane), samuel.legros@cea.fr (S. Legros), geraldine.sarret@ujf-grenoble.fr (G. Sarret).

http://dx.doi.org/10.1016/j.jhazmat.2014.03.014
0304-3894/

1. Introduction

Nanotechnologies are developing rapidly, which is translated by an increasing production of nanomaterials, number of products containing nanomaterials and diversity of these nanomaterials. Among them, titanium dioxide nanoparticles (TiO_2-NPs) are the NPs produced in largest quantities, with between 7800 and 38,000 tons of TiO_2-NPs per year, followed by carbon nanotubes with less than 1000 tons per year [1]. Nanosized TiO_2 has been introduced in a wide range of commercial products for their photocatalytic activity and anti-UV properties: sunscreen, food packaging, sportswear, self-cleaning glass or paints [2]. It is estimated that in 2015, 15–30% of the façade coatings will contain nanomaterials [3].

TiO_2 microparticles (TiO_2-MPs) have been used for several decades for their ability to confer whiteness and opacity to materials. For instance, they are used as an additive in food and pharmaceuticals products under the name E171 (in milk, cheese, sauce, toothpaste or cosmetics) as well as in the building industry as pigment for paints [2]. In all these products no information is provided on the size of the particles. Although these particles are not considered as nanomaterials, they may contain a fraction of particles with a diameter under 100 nm.

A certain proportion of these nanomaterials will be released in the environment [4]. For instance, several studies have demonstrated that TiO_2-NPs contained in textile, cosmetics and nanocomposites will be released in wastewaters [5,6]. After the wastewater treatment, these NPs are expected to accumulate mostly in sewage sludge with a minor proportion being released in effluents [7]. Likewise, TiO_2-NPs contained in paints and concrete are predicted to be released in runoff as particles ranging from 20 to 300 nm under natural weather conditions [8]. Runoff water may be collected by infiltration basins or ends up directly in aquatic systems. Finally, TiO_2-NPs may also be released in the atmosphere upon abrasion (*e.g.* during façade sanding).

TiO_2-NPs can also be introduced intentionally in the environment and deposited directly on crop plants since they are present in some plant protection products and fertilizers [9]. Although the use of NPs in these products is claimed as a way to decrease the total amount of chemicals spread in the field, Gogos et al. [9] estimated that the application of such products could increase fluxes of nanomaterials on soils up to three orders of magnitude as compared to those estimated previously by Mueller and Nowack [10].

The impact of NP dissemination on ecosystems needs to be analyzed. Recent reviews show that most studies in nanoecotoxicology focused on micro-organisms and aquatic organisms [11–15]. The possible transfer of NPs in plants and their phytotoxic effects are less documented, although plants represent a major point of entry of contaminants in the food web and are in direct interaction with air, soil and water [16–18]. Studies on plants were mainly performed by root exposure on plants grown in hydroponics. They showed either positive effects on plant development [19,20], negative effects [21–26] or no effect [27–30]. The uptake of TiO_2-NPs after root exposure has been demonstrated in several studies [29–31].

The impact of TiO_2-NPs on plants after leaf exposure has been much less investigated although this pathway is very likely to occur [12]. A set of studies was performed on spinach after leaf exposure to TiO_2-NPs [32,33]. The authors evidenced enhancement of photosynthetic activity as well as better nitrogen metabolism and an increased biomass production in exposed plantlets. Kurepa et al. showed the internalization of TiO_2-NPs coated with red alizarin S in *Arabidopsis thaliana* leaves after immersing seedlings in a suspension of NPs [31], and Wang et al. observed the disruption of the microtubular network using the same experimental design [22]. A few studies were conducted on crops after foliar exposure to other types of NPs including Au [34], CeO_2 [35] and Ag [36] NPs.

Finally, another aspect that is more and more stressed in nanoecotoxicology is the need to work not only on pristine NPs but also on their aged and transformed by-products which will be released in the environment [28,37,38].

The present study focuses on the fate of pristine TiO_2-NPs and TiO_2-NPs contained in an aged product in crop plants after foliar exposure. Outdoor façade paint, containing both TiO_2-NPs and TiO_2-MPs, was used as aged product after UV exposure and abrasion. Lettuce (*Lactuca sativa*) was chosen as model species because of its widespread occurrence in kitchen gardens and farmlands and large leaf surface making it an ideal model to study the foliar transfer of atmospheric contaminants [36,39,40]. Ti distribution and speciation in lettuce leaves exposed to pristine TiO_2-NPs were studied by a combination of micro-spectroscopic techniques. Ti distribution at the surface, tissue and cellular scales was investigated by time of flight secondary ion mass spectrometry (ToF-SIMS), synchrotron based micro X-ray fluorescence (SR-μXRF), and electron microscopy, respectively. Ti speciation was elucidated by micro X-ray absorption near edge structure spectroscopy (μXANES). Ti total and local concentrations were measured by inductively coupled plasma mass spectrometry (ICP-MS) and micro particle-induced X-ray emission (μPIXE). To assess the impact of pristine TiO_2-NPs on plant development, phytotoxicity markers were analyzed. Additionally, Ti localization and speciation in lettuce leaves exposed to paint leachate were studied by SR-μXRF and μXANES. Summary of the analyses carried out on each sample is available in supporting information (Fig. S1).

2. Materials and methods

2.1. Nanomaterial preparation and characterization

Pristine TiO_2-NPs, pristine TiO_2-MPs and aged paint containing both types of particles were provided by the paint company Materis (Italy). TiO_2-NPs (anatase 4 nm), TiO_2-MPs (rutile ≈ 150 nm) and aged paint (82% rutile, 18% anatase) leachate were fully characterized (see supporting information and Fig. S2).

2.2. Plant culture and exposure

Five young lettuce plantlets (*L. sativa*, var. Laitue Romaine) per condition were grown in compost in a growth chamber (day/night photoperiod 16 h/8 h, day/night temperature 24/20 °C and day/night relative humidity 49/74%) until they reach the five-leaf stage. They were watered with tap water whenever needed.

Before each exposure, stock suspensions were prepared with NPs dispersed in ultrapure water and homogenized 20 min with an ultrasonic bath. Fresh leachate was also generated.

Pristine TiO_2-NP exposure was performed once on the adaxial side of four leaves per plant. Droplets of ultrapure water containing 0.125, 1.25 and 12.5 mmol L^{-1} TiO_2-NPs were deposited on the leaf surface (1 μL per 25 mm^2, *i.e.*, 0.05, 0.5 and 5 nmol TiO_2-NPs mm^{-2}) and then spread all over the surface. This exposure corresponds to a final concentration of approximately 12.5, 125 and 1250 nmol TiO_2-NPs per g^{-1} fresh weight (FW). Likewise for the paint leachate, droplets of 1 μL per 25 mm^2 of foliar surface were deposited on the leaf surface and spread. Since Ti concentration in paint leachate was low, this application was reproduced every day during the exposure time course leading to a final concentration of 35 nmol g^{-1} FW TiO_2. In parallel, control plants were sprayed with ultrapure water using the same protocol. After a 7-day exposure, plantlets were harvested and leaves were thoroughly washed with ultrapure water, gently soaked with a tissue, and fresh foliar biomass was determined. Plant

leaves were then pooled and prepared according to each technique as detailed below.

2.3. Localization and speciation of Ti

2.3.1. Ti distribution by electron microscopy

NP distribution on the leaf surface was investigated by scanning electron microscopy (SEM; Quanta 200, FEI) equipped with energy dispersive X-ray spectroscopy (EDS; X flash 3001 Bruker). Lettuce leaves were oven-dried at 45 °C for 2 days and then mounted on the sample holder without any further preparation. SEM was operated at 15 kV in low vacuum (133 Pa) and in backscattered electron mode. EDS analyses were performed either on spots of interest or in scanning mode.

NP distribution at the cellular scale was investigated on leaf cross-sections prepared by high pressure freezing, cryosubstitution and contrasted with OsO_4 and Pb at the Centre Technologique des Microstructures – UCB Lyon 1. Semi-thin sections (2 μm) were analyzed by SEM-EDS, and ultrathin sections (70 nm) were observed using a TEM (JEOL 1200 EX) operating at 80 kV with an EDS analyzer Kevex.

2.3.2. Ti distribution and speciation by SR-μXRF/μXANES

SR-μXRF and Ti K-edge μXANES measurements were performed in cryo-conditions on ID21 beamline at the ESRF (European Synchrotron Radiation Facility, France) and on LUCIA beamline at SOLEIL (France).

Small pieces of fresh lettuce leaves after washing with deionized water were flash-frozen, embedded in O.C.T.® resin and then cut in thin sections (20 μm) using a cryomicrotome.

SR-μXRF maps were recorded with various step sizes (from 0.3 μm × 0.3 μm to 3 μm × 3 μm) with incident energy of 5.2 keV, and dwell time of 100–2000 ms. SR-μXRF data were fitted using PyMCA software [41]. Ti K-edge μXANES spectra (4.96–5.05 keV energy range, 0.5 eV step) were recorded in regions of interest of the maps with a beam spot of 300 nm × 700 nm. Data treatment and linear combination fitting with a set of reference compounds were performed according to Larue et al. [36] and are detailed in supporting information.

2.3.3. Depth profiling by ToF-SIMS

ToF-SIMS analyses were performed on the surface of lettuce leaves to map Ti-containing molecular fragments using the same procedure as described elsewhere [40]. Ti-rich areas on leaf surface were first localized by SEM. Dried leaf tissue was mounted directly into the sample holder without any further preparation and then examined at room temperature. Positive and negative spectra were obtained on a ToF-SIMS 5 instrument (IONTOF, Münster, Germany) equipped with 25 keV Bi_3^+ primary ion source and a reflectron mass analyzer. The depth profile graph was reconstructed after the normalization of the intensity of the considered mass peaks by calculating the ratio between this intensity and the total intensity measured for each sputtering time (see supporting information for more details).

2.4. Quantitative methods

2.4.1. Total Ti concentration by ICP-MS

The samples were prepared by acid digestion performed in a multiwave 3000 microwave system (Anton Paar, Austria). They were weighed into the Teflon reaction vessel of the microwave and 1 mL of hydrogen peroxide and 2 mL of nitric acid (HNO_3) were added. 15 min later, 5 ml of sulfuric acid were added. The program of mineralization included three stages: (I) from 0 to 800 W during 5 min, (II) 15 min at 800 W ($T = 170 \pm 10$ °C, pressure = 11 ± 3 bar), and (III) 30 min at 0 W. After cooling, the clear solutions obtained were transferred quantitatively into polypropylene tubes, then diluted by a factor of 100 in HNO_3 2%. Blank and diluted pristine TiO_2-NP reference digestions were carried out in the same way (see supporting information).

Total Ti was quantified using an ICP-MS (7700×, Agilent Technologies, Japan). The instrument was calibrated with Ti aqueous reference standards.

2.4.2. Local Ti concentrations by μPIXE

Distribution of endogenous elements (as K and Ca) and Ti was mapped by μPIXE coupled to Rutherford backscattering spectroscopy (RBS) at the AIFIRA nuclear microprobe (Applications Interdisciplinaires de Faisceaux d'Ions en Région Aquitaine, CENBG, France). A 2.5 MeV proton beam was focused to 2.5 μm × 2.5 μm with an average intensity of 1000 pA. At least 3 areas containing epidermis, parenchyma and vein were acquired per sample. Data were processed using SIMNRA [42] and Gupix [43] softwares.

2.5. Phytotoxicity tests

Photosynthetic pigment assay was performed according to Moran et al. [44]. Thiobarbituric acid reactive species (TBARS) were quantified as reported in Dazy et al. [45]. Finally, glutathione (GSH) and phytochelatin (PC) contents were determined by ultra-performance liquid chromatography-tandem mass spectrometry (UPLC MS/MS; Waters UPLC Acquity system coupled to a Waters quadrupole MS/MS Xevo TQD) as detailed in Brautigam et al. [46]. The complete description of these phytotoxicity tests is available in the supporting information. Phytotoxicity tests were carried out on 15 replicates originated from 3 independent experiments.

2.6. Statistical analysis

Statistical analysis was performed using the SigmaStat software with one way ANOVA comparing results obtained for the control plantlets to results obtained in the exposed ones. Significant differences compared to the control were obtained for $p \leq 0.05$ and marked with an asterisk.

3. Results

3.1. Localization of Ti in lettuce leaves

After a 7-day exposure to 1250 nmol g^{-1} FW TiO_2-NPs, lettuce leaves showed Ti-containing particles on their surface and close to stomatal openings as seen by SEM-EDS (Fig. 1A–C). SEM-EDS analyses of leaf cross-sections demonstrated that these particles were also found inside the sub-stomatal chamber (Fig. 1D and F). TEM observations suggested that agglomerates of TiO_2-NPs can damage cuticle and cell walls (Fig. 1E). This effect might be ascribed to the photocatalytic properties of anatase NPs.

Ti distribution in leaf cross-sections was analyzed by SR-μXRF (Fig. 2). XRF spectrum recorded for the plants exposed to 1250 nmol g^{-1} FW TiO_2-NPs showed a sharp peak at the Ti energy (4.5 keV) (Fig. 2H). Ti agglomerates were detected in all types of tissues including epidermis, parenchyma and vascular bundles, with a decreasing concentration from the exposed surface to the inner zones (Figs. 2A–C and S6). From the high resolution map in Fig. 2C, Ti seems to be present both in intercellular and intracellular compartments. Large agglomerates (up to 7 μm × 20 μm) were also evidenced underneath stomata in an area possibly corresponding to the sub-stomatal chamber (Fig. 2A and B). For leaves exposed to aged paint leachate (Fig. 2D and E), although Ti signal was much lower (Fig. 2I), Ti agglomerates were also detected throughout the leaves, and in the apoplasmic and symplasmic compartments. For comparison, a control leaf sprayed with water was analyzed (Fig. 2F

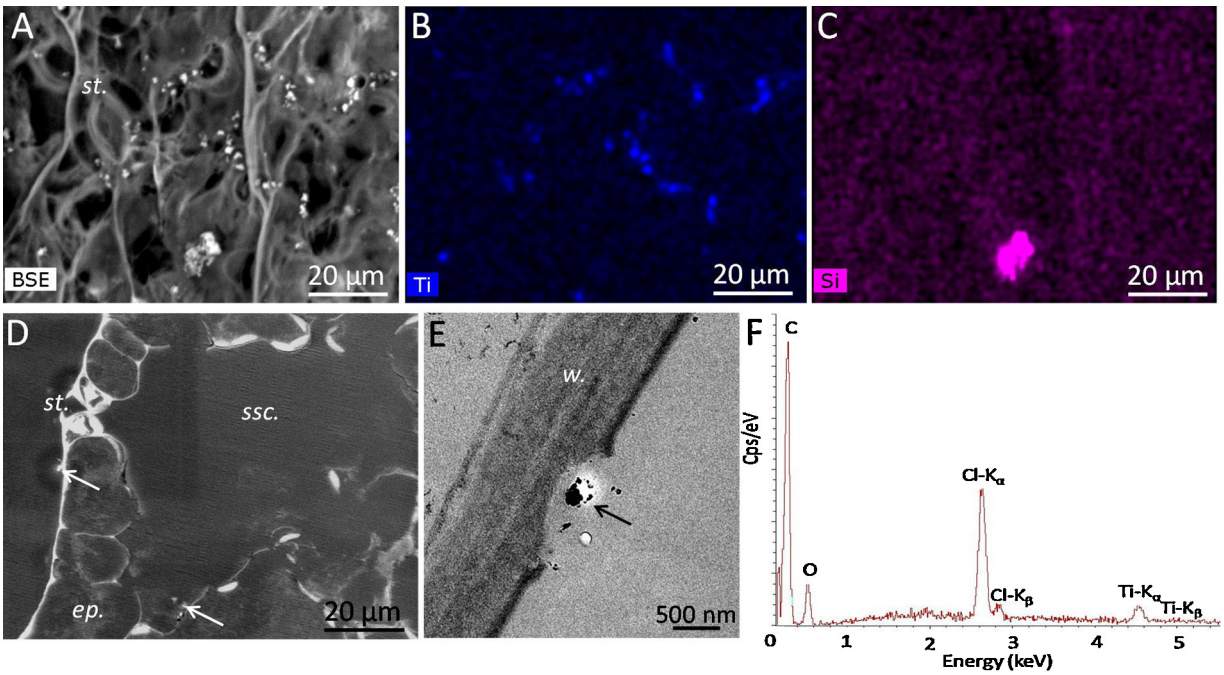

Fig. 1. (A) SEM picture of lettuce leaf exposed to 1250 nmol g^{-1} TiO_2-NPs; EDS analyses of the area in A for Ti (B) and Si (C); SEM (D) and TEM (E) picture of a leaf cross-section; (F) typical EDS spectrum obtained on dots designated by arrows (st., stomata; ep., epidermis; ssc., sub-stomatal cavity; w., wall).

and G). Low intensity Ti signal was detected on single pixels, and a weak Ti peak was present on the total XRF spectrum (Fig. 2J). This low Ti signal may arise from the background Ti contained in the compost growing medium (around 5.5 mmol kg^{-1} DW).

In order to analyze more specifically the interactions between TiO_2-NPs and the leaf surface, lettuce leaves were analyzed by ToF-SIMS depth profiling. In the experimental conditions chosen, the first 200 nm of leaf surface were probed. The results (Fig. 3A and B) clearly show that organic fragment intensity representative of leaf cuticle and/or cuticular wax [47,48] decreased while Ti-containing fragments increased. This observation strongly suggests a trapping of TiO_2-NPs underneath the cuticle/cuticular wax.

3.2. Speciation of Ti in lettuce leaves

To investigate possible chemical transformation of TiO_2-NPs accumulated in leaves, leaf cross-sections were studied by Ti K-edge µXANES spectroscopy. Fig. 4A shows the spectra for reference compounds. The XANES spectra from anatase and rutile differ in the pre-edge with two main pre-peaks for rutile and three for anatase. Moreover, rutile spectrum shows a sharper shoulder on the white line than anatase, and the oscillations after the white line are also different. The spectra for anatase coated with COOH/OH-containing organic compounds present slightly higher pre-peaks and smoother post-edge oscillations as compared to uncoated anatase (Figs. 4A and S7A). COOH/OH-containing molecules may form various types of complexes: monodentate, bidentate, in simple or bridging configurations, as reviewed recently [49]. Two possible types of anatase —COOH containing molecules are shown in Fig. 4B. Considering the nominal diameter of anatase NPs (4 m), one can infer that 31% of atoms are present at the surface (12.5/d, with d the diameter of the particle in angstroms [50]). The presence of organic ligands may modify the geometry of the octahedra present at the surface of NPs, and hence slightly modify the XANES spectrum. A purely Ti-organic complex such as Ti oxalate exhibits clearly different spectral features, with an edge shifted to higher energy, a sharp pre-edge, and smooth post-edge oscillations.

As expected, Ti present inside the leaves after exposure to 1250 nmol g^{-1} TiO_2-NPs had an anatase-like signature (Fig. 4C; Table 1). For most spectra, best linear combination fits were obtained using anatase coated with humic acid (Fig. S7B).

XANES analyses of the aged paint showed a majority of rutile (90%) and a small proportion of anatase particles (11%), which is consistent with the paint formulation (82 and 18%, respectively), with an uncertainty estimated to ±5% for this simple mixture (Fig. 4D; Table 1). The leachate contained about 80% anatase and 20% rutile. Thus, the leaching protocol released more NPs than

Table 1
Ti speciation as determined by linear combination fits of Ti K-edge µXANES spectra.

		Proportion of Ti species (in mol%)			
		TiO_2 rutile	TiO_2 anatase[a]	Sum	NSS (%)[b]
TiO_2-NPs					
Leaf	Spot 1		98	98	0.0003
	Spot 2		88 (6)	88	0.0021
	Spot 3		94	94	0.0033
	Spot 4		102	102	0.0013
	Spot 5		95 (2)	0	0.0056
	Spot 6		108	108	0.0033
	Spot 7		103	103	0.0005
Leachate					
Aged paint		90	11	101	0.0001
Leachate	Spot 1	19 (5)	82 (6)	101	0.0004
	Spot 2	15 (5)	94 (6)	109	0.0003
	Spot 3	31	77	108	0.0003
Epidermis	Spot 1	41 (5)	58 (8)	99	0.0031
Parenchyma	Spot1	104		104	0.0022
	Spot2	111		111	0.0033

[a] Fits were realized with the various anatase species including uncoated anatase 4 nm, anatase 4 nm + humic acid, anatase 4 nm + oxalic acid and anatase 140 nm. When several fits of equivalent quality (increase of NSS < 10%) were obtained with different standards from the "TiO_2 anatase" pool, proportions are expressed as mean percentage (SD) calculated for these fits.

[b] Residual between fit and experimental data: $NSS = \Sigma(\mu_{experimental} - \mu_{fit})^2/\Sigma(\mu_{experimental})^2 \times 100$ in the 4960–5045 eV range.

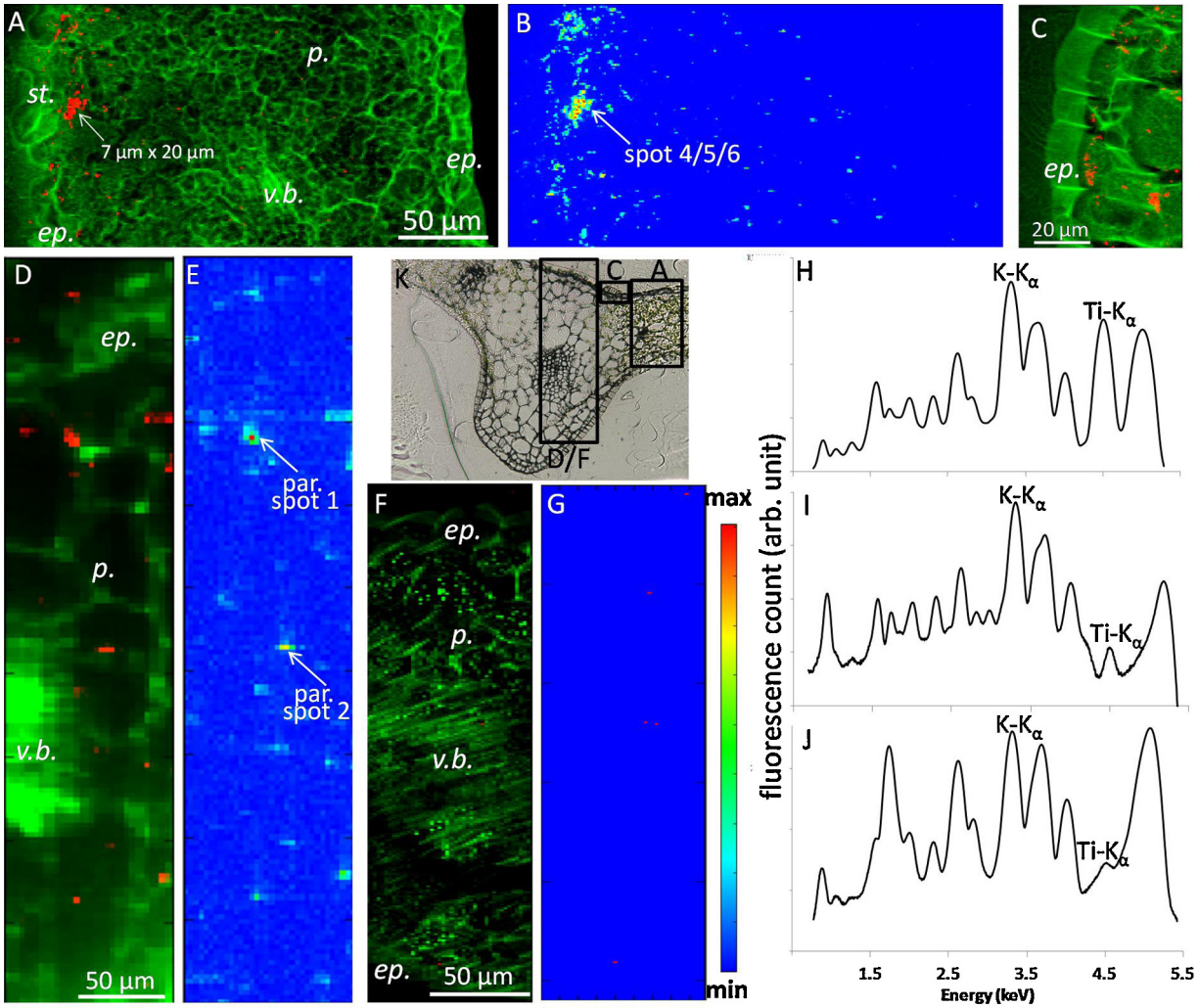

Fig. 2. SR-µXRF maps and spectra for lettuce leaves exposed to 1250 nmol g^{-1} TiO_2-NPs (A, B, C, H), to aged paint leachate (D, E, I) and leaves of control plants sprayed with ultrapure water (F, G, J) (st., stomata; ep., epidermis; p., parenchyma; v.b., vascular bundle). SR-µXRF maps are presented as bicolor maps with K in green and Ti in red (A, C, D, F) and as temperature maps for Ti fluorescence only (B, E, G). Total XRF spectra of maps A, D and F are shown in H–J, respectively. Arrows indicate spots analyzed by µXANES (*cf.* Fig. 5; Table 1). (K) Light microscope picture presenting the localization of the analyzed area. (For interpretation of the references to color in this figure legend, the reader is referred to the web version of this article.)

MPs from the paint matrix. In lettuce leaves exposed to aged paint leachate, both rutile and anatase forms were identified in the tissues. In particular, rutile was identified in the parenchyma. The number of spots analyzed is not sufficient to conclude for a preferential transfer of rutile *vs* anatase, but these results show that not only TiO_2-NPs, but also TiO_2-MPs of 100–200 nm in diameter are able to penetrate inside the leaf tissue.

3.3. Ti total and local concentrations

After foliar exposure to 1250 nmol g^{-1} TiO_2-NPs, the concentration of Ti in/on the contaminated leaves as measured by ICP-MS was significantly higher than in the control plantlets ($p = 0.009$) reaching 630 nmol Ti g^{-1} FW (Fig. 5A), which corresponds to 1050 nmol TiO_2 g^{-1} FW. This can be explain, at least

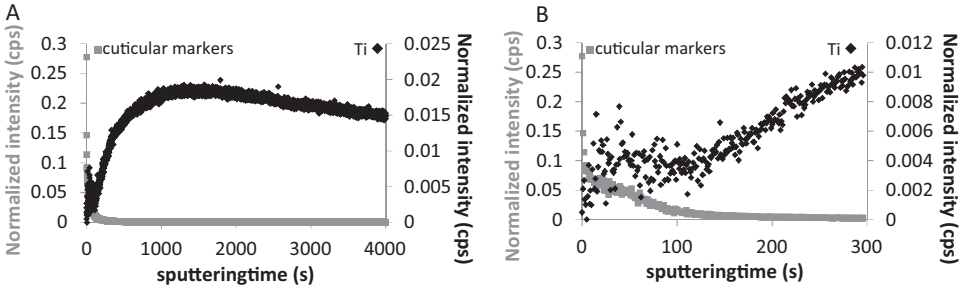

Fig. 3. (A) ToF-SIMS depth profile of lettuce leaves exposed to 1250 nmol g^{-1} TiO_2-NPs. (B) Emphasis on the first 300 s.

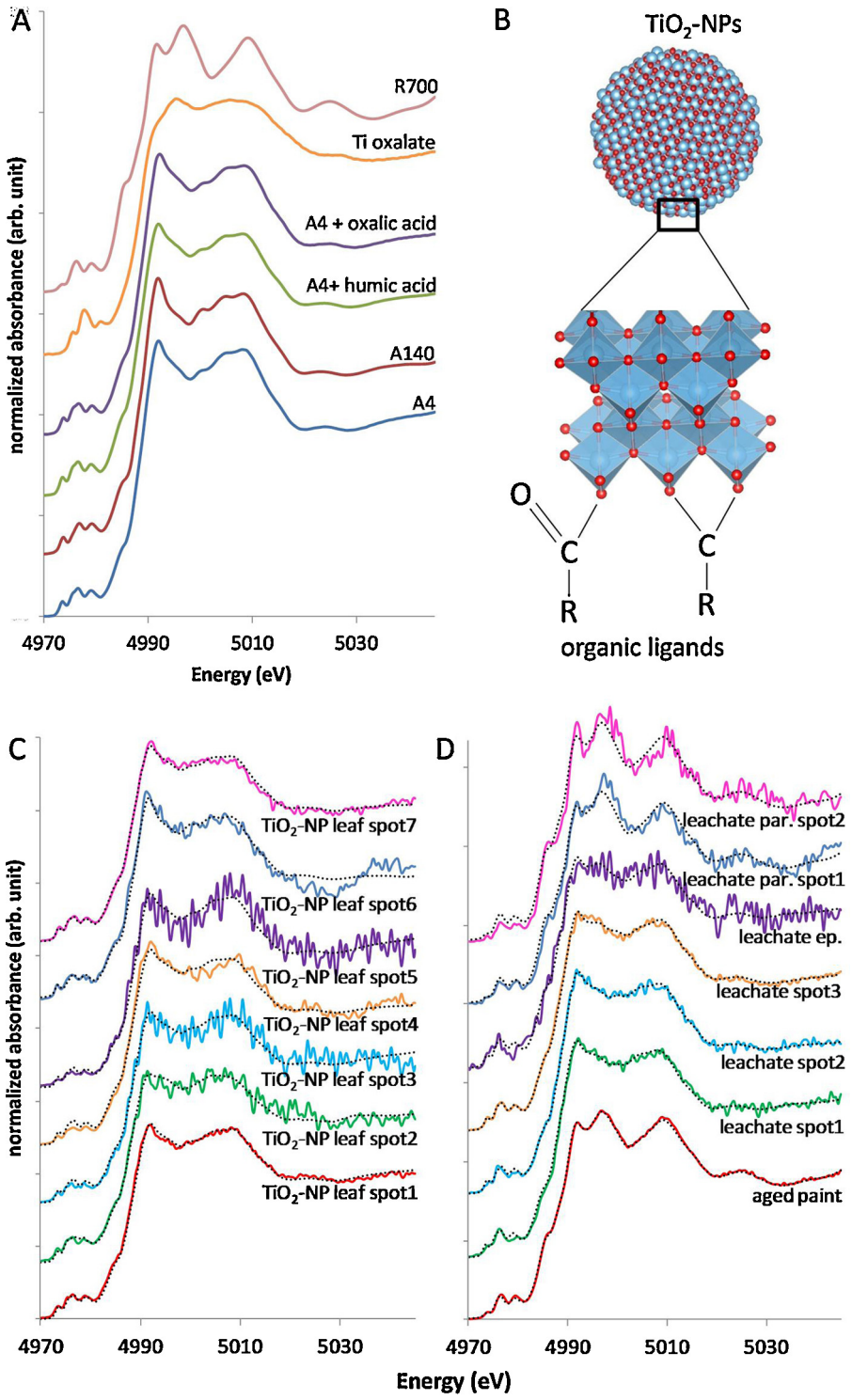

Fig. 4. (A) XANES spectra of the reference compounds; (B) possible interactions between nano anatase surface and organic ligands; μXANES spectra obtained *in situ* on lettuce leaves exposed to 1250 nmol g^{-1} TiO_2-NPs (C) or to aged paint leachate (D). Dotted lines figure the best linear combination fits obtained with reference compounds (par., parenchyma; ep., epidermis; A., anatase; R., rutile).

partly, by a dilution effect due to the growth of leaves during the time course of the exposure. This concentration is in the same range as those measured after foliar exposure of lettuces to Ag-NPs [36], *A. thaliana* seedlings to TiO_2-NPs [31], rapeseed to Au-NPs [34] and maize seedlings to CeO_2-NPs [35]. The control plantlets contained 52 nmol Ti kg^{-1}; this background level comes from naturally occurring Ti in soils. Ti concentration in the compost was 5.5 mmol Ti kg^{-1} DW as measured by ICP-MS.

Local concentrations were then determined by μPIXE/RBS (Fig. 5B–D). In agreement with SR-μXRF results, Ti concentration was highest on the exposed epidermis and decreased progressively going to the abaxial epidermis. Moreover, some very concentrated spots were detected in the epidermis and inside the parenchyma

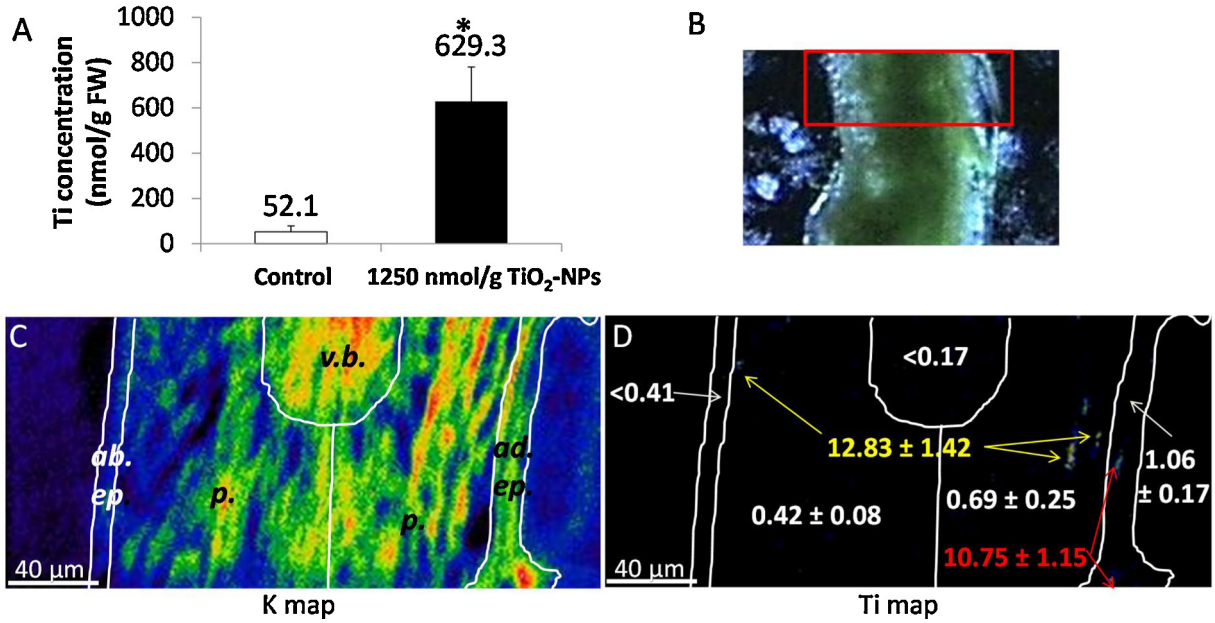

Fig. 5. (A) Ti total concentration in leaves determined by ICP-MS; (B) microscope picture of the area analyzed by µPIXE/RBS on lettuce leaf exposed to 1250 nmol g^{-1} TiO_2-NPs (squared in red); (C) distribution map of K; in white the delimited area for quantification according to tissue type (ab. ep., abaxial epidermis; ad. ep., adaxial epidermis; p., parenchyma; v.b., vascular bundle); (D) Ti distribution map and Ti concentrations (in mmol kg^{-1} dry weight) in each delimitated zone (in white) and in agglomerates designated by red and yellow arrows in the epidermis and parenchyma, respectively. (For interpretation of the references to color in this figure legend, the reader is referred to the web version of this article.)

(up to 12.8 ± 1.4 mmol Ti kg^{-1} DW, as compared to 0.42–1.0 mmol Ti kg^{-1} DW for the whole zones). The lowest concentration was obtained in the vascular bundle. The values obtained by µPIXE/RBS (expressed in DW) are lower than those obtained by ICP-MS (expressed FW). This may arise from heterogeneities in Ti content among plants, leaves and regions of the leaves. Analyses of a larger number of leaf samples by µPIXE/RBS would be required to better assess this heterogeneity. Still, this discrepancy does not preclude the main conclusion of µPIXE/RBS, which is the presence of local Ti concentrations one order of magnitude higher than the average concentration in the considered tissue. For plants exposed to paint leachate, Ti concentration applied was very low

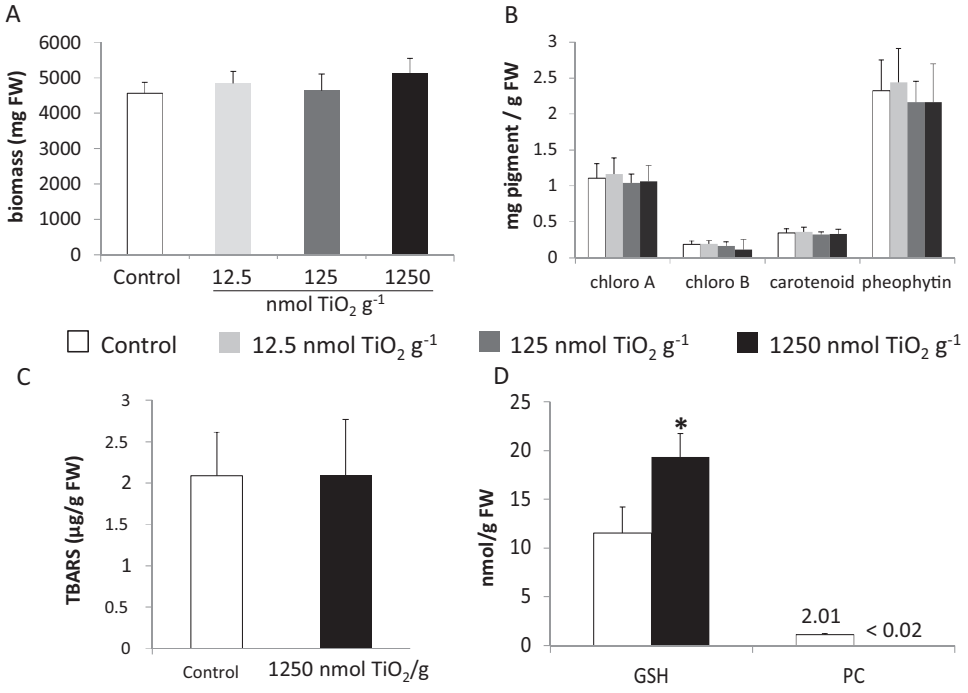

Fig. 6. Phytotoxicity evaluation after a 7-day exposure to pristine TiO_2-NPs. (A) Total foliar biomass; (B) photosynthetic pigment concentration in leaves; (C) lipid peroxidation in leaves assessed by TBARS test; (D) glutathione and phytochelatin concentration in leaves. * indicates significant difference ($p < 0.05$) between the control and the exposed sample.

and thus in the background level of this technique (ppm range [51]).

3.4. Phytotoxicity

Biological markers were investigated to identify a potential impact of pristine TiO_2-NP foliar exposure on lettuces. After a 7-day exposure, the fresh foliar biomass was unchanged regardless of the concentration (Fig. 6A) with a mean biomass of 4796.5 ± 256.3 mg. Chlorophyll *a*, chlorophyll *b*, carotenoid and pheophytin concentrations were not affected by TiO_2-NP exposure (Fig. 6B) with value of 1.094 ± 0.055, 0.164 ± 0.037, 0.339 ± 0.016 and 2.276 ± 0.133 mg pigments g^{-1} FW, respectively. Similarly, TBARS remained unchanged with 2.090 $\mu g\, g^{-1}$ FW in the control plantlets and 2.094 $\mu g\, g^{-1}$ FW for the exposed ones (Fig. 6C).

Concerning thiol-containing compounds, a significant difference ($p = 0.020$) was observed between control (mean 37.4 ± 8.8 nmol g^{-1} FW) and exposed lettuces (mean 63.2 ± 7.8 nmol g^{-1} FW) for GSH concentration (Fig. 6D). Only PC_2 could be detected and quantified in control plants (2.01 ± 0.20 nmol g^{-1} FW), whereas PC was under detection limit in the exposed lettuces (<0.02 nmol g^{-1} FW).

4. Discussion

The present study demonstrates that pristine agglomerated TiO_2-NPs as well as TiO_2-NPs and -MPs from an aged product are taken up by lettuce leaves after being deposited on leaf surface. These particles are observed in the epidermis, parenchyma and vascular tissues, both in the apoplasmic and symplasmic compartments. Concerning the mechanisms underlying NP internalization, our results suggest that NPs may follow both the stomatal and cuticular pathways. TiO_2 agglomerates were detected at the stomatal opening and in the sub-stomatal chamber by SEM-EDS and SR-μXRF. Similar localization was observed in a parallel experiment with lettuces exposed to pristine Ag-NPs [36]. These results are also in agreement with a study performed on *Vicia faba* leaves where 43 nm polystyrene NPs with a hydrophilic coating were detected in the sub-stomatal chamber [52]. More recently, TiO_2-NPs coated with red alizarin S were shown to follow the same stomatal pathway in *A. thaliana* seedlings, but NPs were found in vacuoles of guard cells [31]. An alternative way of entry for NPs is the cuticular pathway. ToF-SIMS analyses supported this hypothesis by showing a trapping of Ti by the cuticle. Moreover TEM-EDS results suggested that TiO_2-NP agglomerates were able to damage cuticle and cell walls. The next barrier for the entry of NPs into cells is the cell membrane. In our experiment, TBARS assay, representative of membrane damaging, did not increase under TiO_2-NP exposure. The internalization of TiO_2-NPs by endocytosis, which was proposed in other studies [29,31] based on the observation of endosomes containing TiO_2-nanocomposites, might explain the absence of detectable damage to cell membranes.

Interestingly, results for plants exposed to paint leachate showed that both 4 nm anatase NPs and rutile MPs larger than 100 nm coming from paint matrix were able to penetrate inside leaves. The paint contains different chemical organic compounds such as surfactants; that might have eased particle internalization. The present study demonstrates that the actual size exclusion limit for TiO_2 particles in lettuce leaves is higher than 100 nm. In the parenchyma, the two spots analyzed by μXANES contained 100% rutile particles. Here, statistics are not sufficient to conclude for a preferential accumulation of rutile *vs* anatase form. However, studies on cucumber plantlets exposed to a mixture of anatase and rutile NPs showed a preferential translocation of rutile NPs in phloem, leaves and fruits [53,54]. Further experiments are necessary to elucidate this point.

Elemental speciation is essential to assess the fate and toxicity of metals in plants. μXANES results for plants exposed to pristine TiO_2-NPs showed that their crystal structure remained unchanged after internalization. This result is consistent with the high stability of TiO_2 crystalline forms, and is in agreement with previous studies [29,53]. The linear combination fitting also suggests the presence of an organic coating around the TiO_2-NPs accumulated in the plant tissues. This could be explained by the strong photocalytic capability of TiO_2 to degrade organic molecules under light. We can hypothesize that when trapped in cuticular wax, degradation of alcohol or fatty acid molecules into lower molecular species may be promoted by TiO_2-NPs leading to the formation of TiO_2-organic complexes. The presence of the nanoparticulate form of TiO_2 in plants sustains the study of the fate of pristine NPs in the gastro-intestinal tract in the scenario of human consumption of contaminated vegetables.

To elucidate NP phytotoxicity after the 7-day exposure, several endpoints were assessed. Foliar exposure to pristine TiO_2-NPs did not lead to noticeable changes in plant fresh foliar biomass, photosynthetic pigment and lipid peroxidation. An increase in GSH content and decrease in PC_2 were observed, but these concentrations were low as compared to typical values in plants: 300 nmol g^{-1} FW for GSH [55]. The use of longer exposure times and finer toxicity markers would be necessary to conclude more firmly on the effect of TiO_2-NPs on lettuce. In a study on *V. faba* after root exposure to aged TiO_2-nanocomposite, Foltete et al. showed no impact on GSH and PCs contents in roots and shoots, and a decrease in glutathione reductase activity in roots [28]. In other studies on spinach, foliar exposure to anatase and rutile TiO_2-NPs enhanced the biomass, protein content and photosynthetic activity [33,56,57]. Finally, in a study on *A. thaliana* after submerging the seedlings in a suspension of anatase TiO_2-NPs coated with alizarine red S, disruption of the microtubular network was observed [22]. This overview of the still very limited knowledge on the phytotoxicity of NPs suggests that these materials induce a larger diversity of effects and responses as compared to metals and metalloid ions, for which the phytotoxicity is much better known.

5. Conclusion

This work supports previous studies showing that NPs can be internalized in plants through foliar pathway. Moreover, it provides new information on size exclusion limit, mechanisms of internalization and sites of bioaccumulation. Pristine NPs as well as NPs and MPs released from aged paint were shown to be transferred inside the leaf tissue, and accumulated both in the extracellular and intracellular compartments. Our results demonstrate that both stomatal and cuticular pathways might be involved in the transfer. The crystalline form of NPs was not modified upon bioaccumulation. The 7-day exposure to pristine TiO_2-NPs did not induce acute phytotoxicity. These results have two major implications. First, transfer in the food chain *via* plants should be considered in the life cycle analysis of NPs, not only through the roots but also through the aerial parts; second, particles larger than the arbitrary 100 nm diameter limit may be transferred to plant tissues as well. These insights are of particular importance for the risk assessment of crop plants exposed to atmospheric contaminants, which is an increasing concern in regions of fast economic growth [58–60].

Acknowledgements

The authors would like to thank the FP7 of the European Union for the funding (Nanohouse project no. 247810) and French

program LABEX Serenade (11-LABX-0064). C. Larue, L. Cecillon and G. Sarret are part of Labex OSUG@2020 (ANR10 LABX56). We acknowledge the European Synchrotron Radiation Facility and SOLEIL synchrotron for provision of beamtime. We are grateful to AIFIRA for providing access to the nuclear microprobe. TEM analyses were performed on the TEM OSIRIS (Nano-Safety Platform, CEA-Grenoble) funded by the Agence Nationale de la Recherche, program 'Investissements d'Avenir', reference ANR-10-EQPX-39, operated by François Saint Antonin. We also acknowledge Nicolas Nuns from the Pôle Régional d'Analyse de Surface and IRENI program for ToF-SIMS measurements.

Appendix A. Supplementary data

Supplementary data associated with this article can be found, in the online version, at http://dx.doi.org/10.1016/j.jhazmat.2014.03.014.

References

[1] C.O. Hendren, X. Mesnard, J. Dröge, M.R. Wiesner, Estimating production data for five engineered nanomaterials as a basis for exposure assessment, Environ. Sci. Technol. 45 (2011) 2562–2569.
[2] M. Skocaj, M. Filipic, J. Petkovic, S. Novak, Titanium dioxide in our everyday life; is it safe? Radiol. Oncol. 45 (2011) 227–247.
[3] C. Som, P. Wick, H. Krug, B. Nowack, Environmental and health effects of nanomaterials in nanotextiles and facade coatings, Environ. Int. 37 (2011) 1131–1142.
[4] K. Aschberger, C. Micheletti, B. Sokull-Klüttgen, F.M. Christensen, Analysis of currently available data for characterising the risk of engineered nanomaterials to the environment and human health – lessons learned from four case studies, Environ. Int. 37 (2011) 1143–1156.
[5] L. Windler, C. Lorenz, N. von Goetz, K. Hungerbühler, M. Amberg, M. Heuberger, B. Nowack, Release of titanium dioxide from textiles during washing, Environ. Sci. Technol. 46 (2012) 8181–8188.
[6] L. Reijnders, The release of TiO_2 and SiO_2 nanoparticles from nanocomposites, Polym. Degrad. Stabil. 94 (2009) 873–876.
[7] M. Kiser, P. Westerhoff, T. Benn, Y. Wang, J. Perez-Rivera, K. Hristovski, Titanium nanomaterial removal and release from wastewater treatment plants, Environ. Sci. Technol. 43 (2009) 6757–6763.
[8] R. Kaegi, A. Ulrich, B. Sinnet, R. Vonbank, A. Wichser, S. Zuleeg, H. Simmler, S. Brunner, H. Vonmont, M. Burkhardt, M. Boller, Synthetic TiO(2) nanoparticle emission from exterior facades into the aquatic environment, Environ. Pollut. 156 (2008) 233–239.
[9] A. Gogos, K. Knauer, T.D. Bucheli, Nanomaterials in plant protection and fertilization: current state, foreseen applications, and research priorities, J. Agric. Food Chem. 60 (2012) 9781–9792.
[10] N.C. Mueller, B. Nowack, Exposure modeling of engineered nanoparticles in the environment, Environ. Sci. Technol. 42 (2008) 4447–4453.
[11] A. Menard, D. Drobne, A. Jemec, Ecotoxicity of nanosized TiO_2. Review of in vivo data, Environ. Pollut. 159 (2011) 677–684.
[12] M.A. Maurer-Jones, I.L. Gunsolus, C.J. Murphy, C.L. Haynes, Toxicity of engineered nanoparticles in the environment, Anal. Chem. 85 (2013) 3036–3049.
[13] J. Fabrega, S.N. Luoma, C.R. Tyler, T.S. Galloway, J.R. Lead, Silver nanoparticles: behaviour and effects in the aquatic environment, Environ. Int. 37 (2011) 517–531.
[14] J.T.K. Quik, J.A. Vonk, S.F. Hansen, A. Baun, D. Van De Meent, How to assess exposure of aquatic organisms to manufactured nanoparticles? Environ. Int. 37 (2011) 1068–1077.
[15] A. Kahru, H.-C. Dubourguier, From ecotoxicology to nanoecotoxicology, Toxicology 269 (2010) 105–119.
[16] P. Miralles, T.L. Church, A.T. Harris, Toxicity, uptake, and translocation of engineered nanomaterials in vascular plants, Environ. Sci. Technol. 46 (2012) 9224–9239.
[17] C.M. Rico, S. Majumdar, M. Duarte-Gardea, J.R. Peralta-Videa, J.L. Gardea-Torresdey, Interaction of nanoparticles with edible plants and their possible implications in the food chain, J. Agric. Food Chem. 59 (2011) 3485–3498.
[18] K.J. Dietz, S. Herth, Plant nanotoxicology, Trends Plant Sci. 16 (2011) 582–589.
[19] H. Feizi, M. Kamali, L. Jafari, P. Rezvani Moghaddam, Phytotoxicity and stimulatory impacts of nanosized and bulk titanium dioxide on fennel (*Foeniculum vulgare* Mill), Chemosphere 91 (2013) 506–511.
[20] D. Singh, S. Kumar, S.C. Singh, B. Lal, N.B. Singh, Applications of liquid assisted pulsed laser ablation synthesized TiO_2 nanoparticles on germination, growth and biochemical parameters of *Brassica oleracea* var. *Capitata*, Sci. Adv. Mater. 4 (2012) 522–531.
[21] S. Asli, P.M. Neumann, Colloidal suspensions of clay or titanium dioxide nanoparticles can inhibit leaf growth and transpiration via physical effects on root water transport, Plant Cell Environ. 32 (2009) 577–584.
[22] S.H.W.S.H. Wang, J. Kurepa, J.A. Smalle, Ultra-small TiO(2) nanoparticles disrupt microtubular networks in *Arabidopsis thaliana*, Plant Cell Environ. 34 (2011) 811–820.
[23] P. Landa, R. Vankova, J. Andrlova, J. Hodek, P. Marsik, H. Storchova, J.C. White, T. Vanek, Nanoparticle-specific changes in *Arabidopsis thaliana* gene expression after exposure to ZnO, TiO_2, and fullerene soot, J. Hazard. Mater. 241/242 (2012) 55–62.
[24] M. Ghosh, M. Bandyopadhyay, A. Mukherjee, Genotoxicity of titanium dioxide (TiO(2)) nanoparticles at two trophic levels Plant and human lymphocytes, Chemosphere 81 (2010) 1253–1262.
[25] K. Klancnik, D. Drobne, J. Valant, J.D. Koce, Use of a modified Allium test with nanoTiO(2), Ecotoxicol. Environ. Saf. 74 (2011) 85–92.
[26] M. Ruffini Castiglione, L. Giorgetti, C. Geri, R. Cremonini, The effects of nano-TiO_2 on seed germination, development and mitosis of root tip cells of *Vicia narbonensis* L. and *Zea mays* L., J. Nanopart. Res. 13 (2011) 2443–2449.
[27] E. Seeger, A. Baun, M. Kastner, S. Trapp, Insignificant acute toxicity of TiO_2 nanoparticles to willow trees, J. Soils Sedim. 9 (2009) 46–53.
[28] A.S. Foltete, J.F. Masfaraud, E. Bigorgne, J. Nahmani, P. Chaurand, C. Botta, J. Labille, J. Rose, J.F. Ferard, S. Cotelle, Environmental impact of sunscreen nanomaterials: ecotoxicity and genotoxicity of altered TiO_2 nanocomposites on *Vicia faba*, Environ. Pollut. 159 (2011) 2515–2522.
[29] C. Larue, J. Laurette, N. Herlin-Boime, H. Khodja, B. Fayard, A.M. Flank, F. Brisset, M. Carriere, Accumulation, translocation and impact of TiO_2 nanoparticles in wheat (*Triticum aestivum* spp.): influence of diameter and crystal phase, Sci. Total Environ. 431 (2012) 197–208.
[30] C. Larue, G. Veronesi, A.M. Flank, S. Surble, N. Herlin-Boime, M. Carriere, Comparative uptake and impact of TiO(2) nanoparticles in wheat and rapeseed, J. Toxicol. Environ. Health A 75 (2012) 722–734.
[31] J. Kurepa, T. Paunesku, S. Vogt, H. Arora, B.M. Rabatic, J.J. Lu, M.B. Wanzer, G.E. Woloschak, J.A. Smalle, Uptake and distribution of ultrasmall anatase TiO(2) alizarin red S nanoconjugates in *Arabidopsis thaliana*, Nano Lett. 10 (2010) 2296–2302.
[32] Z. Lei, M.Y. Su, L. Chao, C. Liang, H. Hao, W. Xiao, X.Q. Liu, Y. Fan, F.Q. Gao, F.S. Hong, Effects of nanoanatase TiO_2 on photosynthesis of spinach chloroplasts under different light illumination, Biol. Trace Elem. Res. 119 (2007) 68–76.
[33] F. Yang, F.S. Hong, W.J. You, C. Liu, F.Q. Gao, C. Wu, P. Yang, Influences of nanoanatase TiO_2 on the nitrogen metabolism of growing spinach, Biol. Trace Elem. Res. 110 (2006) 179–190.
[34] S. Arora, P. Sharma, S. Kumar, R. Nayan, P.K. Khanna, M.G.H. Zaidi, Gold-nanoparticle induced enhancement in growth and seed yield of *Brassica juncea*, Plant Growth Regul. 66 (2012) 303–310.
[35] K. Birbaum, R. Brogioli, M. Schellenberg, E. Martinoia, W.J. Stark, D. Gunther, L.K. Limbach, No evidence for cerium dioxide nanoparticle translocation in maize plants, Environ. Sci. Technol. 44 (2010) 8718–8723.
[36] C. Larue, H. Castillo-Michel, S. Sobanska, L. Cécillon, S. Bureau, V. Barthès, L. Ouerdane, M. Carrière, G. Sarret, Foliar exposure of the crop *Lactuca sativa* to silver nanoparticles: evidence for internalization and changes in Ag speciation, J. Hazard. Mater. 264 (2014) 98–106.
[37] E. Bigorgne, L. Foucaud, E. Lapied, J. Labille, C. Botta, C. Sirguey, J. Falla, J. Rose, E.J. Joner, F. Rodius, J. Nahmani, Ecotoxicological assessment of TiO_2 byproducts on the earthworm *Eisenia fetida*, Environ. Pollut. 159 (2011) 2698–2705.
[38] E. Lapied, J.Y. Nahmani, E. Moudilou, P. Chaurand, J. Labille, J. Rose, J.M. Exbrayat, D.H. Oughton, E.J. Joner, Ecotoxicological effects of an aged TiO_2 nanocomposite measured as apoptosis in the anecic earthworm *Lumbricus terrestris* after exposure through water, food and soil, Environ. Int. 37 (2011) 1105–1110.
[39] G. Uzu, S. Sobanska, G. Sarret, M. Munoz, C. Dumat, Foliar lead uptake by lettuce exposed to atmospheric fallouts, Environ. Sci. Technol. 44 (2010) 1036–1042.
[40] E. Schreck, Y. Foucault, G. Sarret, S. Sobanska, L. Cécillon, M. Castrec-Rouelle, G. Uzu, C. Dumat, Metal and metalloid foliar uptake by various plant species exposed to atmospheric industrial fallout: mechanisms involved for lead, Sci. Total Environ. 427/428 (2012) 253–262.
[41] V.A. Sole, E. Papillon, M. Cotte, P. Walter, J. Susini, A multiplatform code for the analysis of energy-dispersive X-ray fluorescence spectra, Spectrochim. Acta Part B: Atomic Spectrosc. 62 (2007) 63–68.
[42] M. Mayer, SIMNRA, a simulation program for the analysis of NRA, RBS and ERDA, Appl. Accelerators Res. Ind. 475 (Pts 1 and 2) (1999) 541–544.
[43] J.L. Campbell, T.L. Hopman, J.A. Maxwell, Z. Nejedly, The Guelph PIXE software package III: alternative proton database, Nucl. Instrum. Methods Phys. Res., Sect. B 170 (2000) 193–204.
[44] R. Moran, Formulas for determination of chlorophyllous pigments extracted with N,N-dimethylformamide, Plant Physiol. 69 (1982) 1376–1381.
[45] M. Dazy, V. Jung, J.F. Ferard, J.F. Masfaraud, Ecological recovery of vegetation on a coke-factory soil: role of plant antioxidant enzymes and possible implications in site restoration, Chemosphere 74 (2008) 57–63.
[46] A. Brautigam, D. Wesenberg, H. Preud'homme, D. Schaumloffel, Rapid and simple UPLC–MS/MS method for precise phytochelatin quantification in alga extracts, Anal. Bioanal. Chem. 398 (2010) 877–883.
[47] R. Jetter, R. Sodhi, Chemical composition and microstructure of waxy plant surfaces: triterpenoids and fatty acid derivatives on leaves of *Kalanchoe daigremontiana*, Surf. Interface Anal. 43 (2011) 326–330.
[48] M.C. Perkins, C.J. Roberts, D. Briggs, M.C. Davies, A. Friedmann, C.A. Hart, G.A. Bell, Surface morphology and chemistry of *Prunus laurocerasus* L. leaves: a study using X-ray photoelectron spectroscopy, time-of-flight secondary-ion mass spectrometry, atomic-force microscopy and scanning-electron microscopy, Planta 221 (2005) 123–134.

[49] A.G. Thomas, K.L. Syres, Adsorption of organic molecules on rutile TiO_2 and anatase TiO_2 single crystal surfaces, Chem. Soc. Rev. 41 (2012) 4207–4217.
[50] L.X. Chen, T. Rajh, Z. Wang, M.C. Thurnauer, XAFS studies of surface structures of tio2 nanoparticles and photocatalytic reduction of metal ions, J. Phys. Chem. B 101 (1997) 10688–10697.
[51] E. Lombi, G.M. Hettiarachchi, K.G. Scheckel, Advanced in situ spectroscopic techniques and their applications in environmental biogeochemistry: introduction to the special section, J. Environ. Qual. 40 (2011) 659–666.
[52] T. Eichert, A. Kurtz, U. Steiner, H.E. Goldbach, Size exclusion limits and lateral heterogeneity of the stomatal foliar uptake pathway for aqueous solutes and water-suspended nanoparticles, Physiol. Plant. 134 (2008) 151–160.
[53] A.D. Servin, H. Castillo-Michel, J.A. Hernandez-Viezcas, B.C. Diaz, J.R. Peralta-Videa, J.L. Gardea-Torresdey, Synchrotron micro-XRF and micro-XANES confirmation of the uptake and translocation of TiO_2 nanoparticles in cucumber (*Cucumis sativus*) plants, Environ. Sci. Technol. 46 (2012) 7637–7643.
[54] A.D. Servin, M.I. Morales, H. Castillo-Michel, J.A. Hernandez-Viezcas, B. Munoz, L. Zhao, J.E. Nunez, J.R. Peralta-Videa, J.L. Gardea-Torresdey, Synchrotron verification of TiO_2 accumulation in cucumber fruit: a possible pathway of TiO_2 nanoparticle transfer from soil into the food chain, Environ. Sci. Technol. 47 (2013) 11592–11598.
[55] G. Noctor, A. Mhamdi, S. Chaouch, Y. Han, J. Neukermans, B. Marquez-Garcia, G. Queval, C.H. Foyer, Glutathione in plants: an integrated overview, Plant Cell Environ. 35 (2012) 454–484.
[56] F.Q. Gao, F.H. Hong, C. Liu, L. Zheng, M.Y. Su, X. Wu, F. Yang, C. Wu, P. Yang, Mechanism of nano-anatase TiO_2 on promoting photosynthetic carbon reaction of spinach-inducing complex of Rubisco–Rubisco activase, Biol. Trace Elem. Res. 111 (2006) 239–253.
[57] L. Zheng, F.S. Hong, S.P. Lu, C. Liu, Effect of nano-TiO_2 on strength of naturally and growth aged seeds of spinach, Biol. Trace Elem. Res. 104 (2005) 83–91.
[58] A. Lapresta-Fernández, A. Fernández, J. Blasco, Public concern over ecotoxicology risks from nanomaterials: pressing need for research-based information, Environ. Int. 39 (2012) 148–149.
[59] J. Feng, Y. Wang, J. Zhao, L. Zhu, X. Bian, W. Zhang, Source attributions of heavy metals in rice plant along highway in Eastern China, J. Environ. Sci. (China) 23 (2011) 1158–1164.
[60] R. Pandey, K. Shubhashish, J. Pandey, Dietary intake of pollutant aerosols via vegetables influenced by atmospheric deposition and wastewater irrigation, Ecotoxicol. Environ. Saf. 76 (2012) 200–208.